

See discussions, stats, and author profiles for this publication at: <https://www.researchgate.net/publication/274900823>

# Photoionization of Benzophenone in the Gas Phase: Theory and Experiment

ARTICLE in THE JOURNAL OF PHYSICAL CHEMISTRY A · APRIL 2015

Impact Factor: 2.69 · DOI: 10.1021/acs.jpca.5b02706 · Source: PubMed

CITATION

1

READS

106

10 AUTHORS, INCLUDING:



**Sabri Messaoudi**

Faculté des Sciences de Bizerte, Bizerte, Tunisia

28 PUBLICATIONS 257 CITATIONS

SEE PROFILE



**Manef Abderrabba**

Université Paris-Sud 11

165 PUBLICATIONS 1,193 CITATIONS

SEE PROFILE



**Majdi Hochlaf**

Université Paris-Est Marne-la-Vallée

240 PUBLICATIONS 1,592 CITATIONS

SEE PROFILE



**Lionel Poisson**

French National Centre for Scientific Research

106 PUBLICATIONS 929 CITATIONS

SEE PROFILE

# Photoionization of Benzophenone in the Gas Phase: Theory and Experiment

Noura Khemiri,<sup>†</sup> Sabri Messaoudi,<sup>†</sup> Manef Abderrabba,<sup>†</sup> Gloria Spighi,<sup>‡</sup> Marc-André Gaveau,<sup>‡</sup> Marc Briant,<sup>‡</sup> Benoît Soep,<sup>§</sup> Jean-Michel Mestdag,<sup>§</sup> Majdi Hochlaf,<sup>\*,||</sup> and Lionel Poisson<sup>\*,§</sup>

<sup>†</sup>Laboratoire Matériaux, Molécules et Applications, Institut Préparatoire aux Etudes Scientifiques et Techniques, La Marsa, Université de Carthage, Carthage, Tunisie

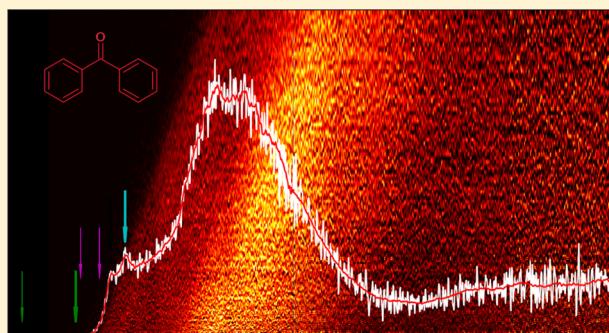
<sup>‡</sup>CEA, CNRS, IRAMIS/LIDyL/Laboratoire Francis Perrin URA2453, CEA Saclay, 91191 Gif-sur-Yvette, France

<sup>§</sup>CNRS, CEA, IRAMIS/LIDyL/Laboratoire Francis Perrin URA2453, CEA Saclay, 91191 Gif-sur-Yvette, France

<sup>||</sup>Université Paris-Est, Laboratoire Modélisation et Simulation Multi Echelle, MSME UMR 8208 CNRS, 5 bd Descartes, 77454 Marne-la-Vallée, France

## S Supporting Information

**ABSTRACT:** We report on the single photoionization of jet-cooled benzophenone using a tunable source of VUV synchrotron radiation coupled with a photoion/photoelectron coincidence acquisition device. The assignment and the interpretation of the spectra are based on a characterization by ab initio and density functional theory calculations of the geometry and of the electronic states of the cation. The absence of structures in the slow photoelectron spectrum is explained by a congestion of the spectrum due to the dense vibrational progressions of the very low frequency torsional mode in the cation either in pure form or in combination bands. Also a high density of electronic states has been found in the cation. Presently, we estimate the experimental adiabatic and vertical ionization energy of benzophenone at  $8.80 \pm 0.01$  and  $8.878 \pm 0.005$  eV, respectively. The ionization energy as well as the energies of the excited states are compared to the calculated ones.



## INTRODUCTION

Neutral benzophenone (Figure 1) is a paradigmatic organic molecule for its triplet dynamics<sup>1–3</sup> and reactivity. For this

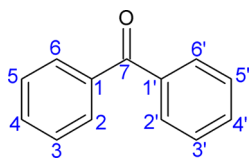


Figure 1. Benzophenone molecule.

specific behavior, benzophenone and close-by structures are used in organic chemistry as a transmitter of triplet excitation to various molecules.<sup>4,5</sup> Its specificity is to combine a strong absorption cross section in the UV with one of the most efficient intersystem crossing within a time scale of a few picoseconds. Such a behavior has stimulated numerous theoretical studies.<sup>6–8</sup> This triplet efficiency stems from a strong spin–orbit coupling and a near degeneracy of excited singlet and triplet states. This arises from the nature of the conjugation of the electrons between the two benzene rings and the carbonyl.<sup>9</sup> The molecule is nonplanar due to steric repulsion between two adjacent hydrogen atoms 2 and 2' of

the two phenyl rings (Figure 1). The electron delocalization depends strongly upon the planarity and will be different in each excited state affecting its energy and couplings. The most extreme case will be found here when benzophenone will be ionized. For fully understanding this complex ionization dynamics, one requires the full characterization of the electronic excited states of neutral benzophenone and also of the cationic species (monomer and fragments). Indeed, state-of-the-art fast and ultrafast experiments end on cation as the probe (see, for instance, ref 3). Nevertheless, very little is known about the cation because it received little attention.<sup>10,11</sup> Most of the previous works were published before 1980. These works allowed a rough estimation of the ionization energy of benzophenone and the thresholds of the main fragmentation channels. For instance, these energies were measured with earlier techniques, where the results are associated with relatively large error bars or indeterminations.

The purpose of the present study is to remediate to this lack. Indeed, we performed single photon ionization of benzophe-

**Special Issue:** Jean-Michel Mestdag Festschrift

**Received:** March 20, 2015

**Revised:** April 2, 2015

none using VUV synchrotron radiation coupled to a state-of-the-art electron–ion coincidence experiment. The spectrum is composed of large bands that were assigned on the basis of the present *ab initio* and density functional theory computations. The thresholds for the formation of benzophenone cation and for the dissociative photoionization were determined precisely.

## TECHNICAL SECTION

**Experimental Method.** The present experiments were performed using the SAPHIRS experimental setup equipped with the DELICIOUS III spectrometer,<sup>12</sup> which is installed at the DESIRS<sup>13</sup> beamline of the SOLEIL French Synchrotron facility. This setup has been described extensively in previous works.<sup>14</sup> Shortly, the VUV-light generated by the undulator of this beamline is filtered for high harmonics above 15 eV by an argon gas filter located upstream in the main chamber.<sup>15</sup> Then the light goes through a 200 grooves/mm grating monochromator with 200  $\mu\text{m}$  entrance and output slits to yield a typical 7.5 meV resolution.

The benzophenone molecule placed in a temperature controlled oven at 90° is seeded in helium or argon as carrier gases. A continuous supersonic expansion through a 30  $\mu\text{m}$  diameter nozzle generates a cold free jet. The latter is skimmed and the resulting molecular beam enters the ionization chamber where it crosses the synchrotron beam at a right angle.

Here, we have focused on the mass–photoelectron energy correlation. The photoelectrons and photoions were detected in coincidence and analyzed in mass and energy by the DELICIOUS III double imaging coincidence spectrometer. The resulting photoelectron images were inverted using the pBASEX<sup>16</sup> method. The data collected were compiled for each mass into a matrix and analyzed according to the slow photoelectron spectroscopy (SPES) method.<sup>17–20</sup>

**Theoretical Methods.** The main aim of the present computations is to provide an interpretation of the experimental results. These computations involve the geometry optimizations, the derivation of the ionization energies and of the pattern of the electronic states of the benzophenone cation. In this process, we have optimized the geometries of neutral and ionized benzophenone. First, these structures were computed with the PBE0 density functional method (DFT)<sup>21</sup> as implemented in the GAUSSIAN<sup>22</sup> package. Here, the electron densities of the atoms were described using the aug-cc-pVTZ basis set of Dunning and co-workers.<sup>23,24</sup> We also calculated the harmonic frequencies of the obtained molecular structures to check whether they correspond to minima or transition states. Anharmonic frequencies were computed for the neutral ground state molecule. All calculations were carried out in the  $C_1$  point group. Furthermore, we carried out computations using the Møller–Plesset<sup>25</sup> ((R)MP2 with cc-pVTZ basis-set) or the coupled cluster approach in the single and double approximation with a perturbative treatment of the triple excitations (i.e., (R)CCSD(T)<sup>26–30</sup> with the aug-cc-pVTZ basis set), as implemented in the MOLPRO<sup>31</sup> package. These computations used the PBE0/aug-cc-pVTZ optimized structures as a starting point and the atoms were described using Dunning and co-workers basis sets.<sup>23,24</sup>

The excited electronic states of the benzophenone cation have been also investigated. To this end, we have used the state-averaged multiconfigurational CASSCF<sup>32,33</sup> method followed by the internally contracted multireferential configuration interaction method (MRCI<sup>34,35</sup>) as implemented in the MOLPRO<sup>31</sup> package. This allowed the determination of the

energies of the first eight doublet states of the benzophenone cation. We used active spaces of various sizes: the first one (referred hereafter as “active space 1”) is composed of 8 active molecular orbitals (from HOMO–3 to LUMO+3) and the second one (referred as “active space 2”) is composed of 10 active MOs (from HOMO–4 to LUMO+4). Both active spaces lead to a pattern of close electronic states (Table 4). Therefore, we used active space 1 for the MRCI calculations, where all configurations state functions (CSFs) from the CASSCF wave functions were considered as a reference. The decomposition of the wave functions issued from this calculation is given in Table 5.

## RESULTS AND DISCUSSION

**Structure of the Neutral and Ionic Benzophenone.** To validate the DFT calculations, we first optimized the ground state of the benzophenone geometry and we have compared the results with existing experimental data and previous theoretical calculations.<sup>6–10,36</sup> The ground state benzophenone cation has been calculated with the PBE0 functional and the aug-cc-pVTZ basis set, as the neutral molecule. The optimized structures are shown in Figure 2 and the structural parameters

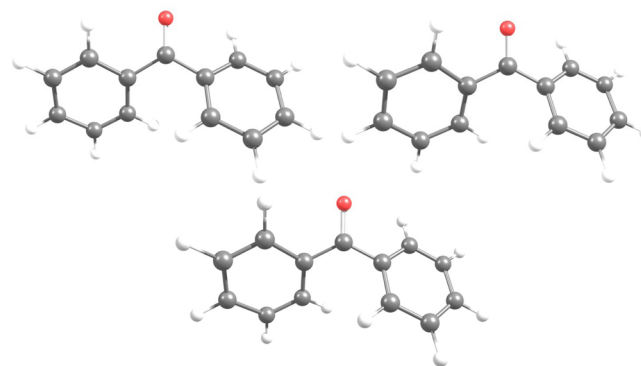


**Figure 2.** Optimized equilibrium geometry of the ground neutral (top-left, DFT/PBE0/aug-cc-pVTZ), ground ionic (top-right, DFT/PBE0/aug-cc-pVTZ) and first ionic excited states (bottom, MP2/aug-cc-pVTZ) of the benzophenone molecule.

are listed in Table 1. After comparison,<sup>8,36</sup> we find a close agreement with experimental data, because deviations are less than 1%. Observing Figure 2 and comparing the bond lengths and angles in neutral benzophenone, it appears that the molecule is of  $C_2$  symmetry but nonplanar. The harmonic and anharmonic frequencies are listed in Table SM-1 (Supporting Information). There are low torsional frequency vibrations of 43  $\text{cm}^{-1}$  indicating a non rigid molecule. This is a priori counterintuitive because conjugation should ensure planarity, but Hoffman and Swenson<sup>7</sup> showed that the repulsion of hydrogen atoms 2 and 2' (Figure 1) twists the ground state molecule to  $\approx 30^\circ$ . We confirm these findings by a twist dihedral angle between the two cycles of  $28^\circ$ . The harmonic and anharmonic frequencies of the stable benzophenone ion are summarized in Table SM-1 (Supporting Information). Similarly to neutral benzophenone, low frequency torsional modes are found making the ion nonrigid with respect to the  $\text{C}=\text{CO}=\text{C}$  torsion.

An important finding of this study is that the bond lengths differ on both sides of the carbonyl cation (Table 1). They are respectively 1.434 and 1.491 Å, whereas the distances are identical in the neutral (1.492 Å) yielding a symmetrical

**Table 1.** Geometry of the Ground State Benzophenone Molecule Neutral  $S_0$  and Ion  $D_0$  and Its First Ion Excited State  $D_1$ . For details of the calculation, see text. Labels of the atoms are given in Figure 1

bond	distance (Å)			angle	(deg)		
	$S_0^a$	ion $D_0$	ion $D_1$		$S_0^a$	ion $D_0$	ion $D_1$
$C_1-C_7$	1.492 (1.48)	1.434	1.453	$C_1-\widehat{C_7}-C_{1'}$	119.8 (122)	127.2	126.1
$C_{1'}-C_7$	1.492 (1.50)	1.491	1.453	$C_6-\widehat{C_1}-C_7=O$	28.2 (56/2)	5.6	29.3
$C_7=O$	1.214 (1.23)	1.228	1.275	$C_6-\widehat{C_{1'}}-C_7=O$	28.2 (56/2)	59.3	29.3
$C_1-C_2$	1.393 (1.40)	1.400	1.422	$C_1-\widehat{C_7}=O$	120.1 (–)	116.9	117.0
$C_{1'}-C_{2'}$	1.393 (1.40)	1.404	1.422	$C_{1'}-\widehat{C_7}=O$	120.1 (–)	116.9	117.0
$C_2-C_3$	1.387 (1.40)	1.380	1.400	$C_6-\widehat{C_1}-C_7$	118.0 (–)	117.2	119.6
$C_{2'}-C_{3'}$	1.387 (1.40)	1.374	1.401	$C_6-\widehat{C_{1'}}-C_7$	118.0 (–)	117.5	119.6
$C_3-C_4$	1.387 (1.36)	1.390	1.411				
$C_{3'}-C_{4'}$	1.387 (1.36)	1.404	1.411				
$C_4-C_5$	1.389 (1.38)	1.393	1.411				
$C_{4'}-C_{5'}$	1.389 (1.37)	1.392	1.411				
$C_5-C_6$	1.383 (1.41)	1.377	1.400				
$C_{5'}-C_{6'}$	1.383 (1.41)	1.377	1.400				
$C_6-C_1$	1.394 (1.40)	1.404	1.422				
$C_{6'}-C_{1'}$	1.394 (1.40)	1.410	1.422				

<sup>a</sup>Between parentheses we give the experimental values from ref 36, distances are given within  $\pm 0.01$  Å, and angles are given within  $\pm 1^\circ$ .

molecule. Thus, the cation is nonsymmetrical. The C=O bond in the ion is 1.228 Å, thus longer than in the neutral molecule 1.214 Å. The angles around the carbonyl group change as well: in the ion, the C=O bond is almost in the plane defined by the closest ring, whereas it was between the two cycles in the neutral; i.e., it turns from about  $23^\circ$ . Meanwhile, the sum of the two dihedral angles along the  $C_1-C_7$  and  $C_{1'}-C_7$  bonds increases by  $10^\circ$  when the ion is compared to the neutral. Thus, the symmetry of the cation is  $C_1$  and when we constrained it to the  $C_2$  symmetry similar to that of the neutral, the system became unstable with an imaginary frequency. Such chemical modifications are observed also when the harmonic frequencies of the neutral molecule and the one of its ions are compared. Indeed, the C=O stretch (mode 11) decreases from 1753 to  $1663\text{ cm}^{-1}$ , and the C—C stretches around the C=O (modes 13 and 15) fall respectively from 1662 to  $1604\text{ cm}^{-1}$  and from 1642 to  $1561\text{ cm}^{-1}$ . The structure of the cation is converging to the delocalization of the charge initially on O atom over the phenyl ring, ensuring a C=O— $\Phi$  planar structure and preserving the full aromaticity of the other ring. We have not found in the literature such examples reported for asymmetric ionic structures in an initially symmetric molecule in its neutral ground state.

On neutral molecules, the question of unequal bond lengths in symmetric molecules like  $\text{NO}_2$  with unequal NO lengths has been a subject of active and contradictory research<sup>37,38</sup> as to what is the best first-order description of the geometry in high lying electronic states? The debate seems closed with the recent calculations of Shinke et al.<sup>39</sup> who assign a symmetric shape to the O—N—O surface in the  $3^2A$ ,  $2^2B_2$  thus in  $C_{2v}$  excited state. Therefore, there are few examples of such an asymmetric surface of great interest in an organic molecule, especially the one having an H-bond involved in their structure, like the acetylacetone molecule<sup>40,41</sup> where the  $C_s$  structure becomes  $C_{2v}$  in the  $S_2$  state.

Thus, these strong structural changes between the neutral and the ion indicate that the Franck–Condon projection for the ionization is poor and may not be efficient enough to reach the adiabatic energy of the ion.

The optimized structure of the first excited state of the ion is displayed in Figure 2. It was optimized at the MP2 level, using the aug-cc-pVTZ basis set. The symmetry group of the molecule is  $C_2$  (calculated in the  $C_1$  symmetry group), similar to the neutral ground state, but with some strong differences in the lengths especially for the C=O bond, which is enlarged to 1.275 Å. One can notice that the C—C distances of the rings are larger than the one of the neutral and ionic ground state.

**Single Photoionization of Benzophenone.** The threshold for ionization has been investigated on supersonically cooled benzophenone at about 30 K<sup>17</sup> by scanning the monochromatic wavelength of the DESIRS beamline and reconstructing the photoelectron spectrum in coincidence with the ion mass at 182 amu. In Figure 3, the photoelectron signal limited to the first 0.45 eV electron kinetic energies is presented in the 8.7–11.0 eV photon range. The SPES spectrum limited to electrons having 0–0.1 eV of kinetic energies is also presented in Figure 3. The shape of the He–I photoelectron spectrum of Centineo et al.<sup>10</sup> fits well the present SPES spectrum. The vertical ionization energy (VIE) is measured as the maximum of the first bump of the SPES signal, at the top of the sharp rise observed (Figure 3). We measure it here as  $8.923 \pm 0.005$  eV (black arrow in the inset of Figure 3).

The absence of a clear 0–0 transition, confirms an apparent unfavorable Franck–Condon overlap between the ground state neutral and the ground state ion. For this reason, the ionization threshold is obtained by linearly extrapolating the rise of the SPES spectrum. The experimental value obtained here is  $8.878 \pm 0.005$  eV (right magenta arrow in the inset of Figure 3) considering the sharp rise as shown in Figure 3, or  $8.80 \pm 0.01$  eV (left magenta arrow in the inset of Figure 3) considering the tail before the rise where electrons ejected from higher photon energies<sup>18</sup> are contributing, thereby approaching the adiabatic ionization energy (AIE). This tail is usually considered as a hot band. Nevertheless, we fit it here because of the apparent lowering of the Franck–Condon factors. Strictly speaking, the AIE cannot be considered as unambiguously determined. Other AIE determination approaches (e.g., ref 42) may lead to lowering to the experimental AIE. An upper bound is given



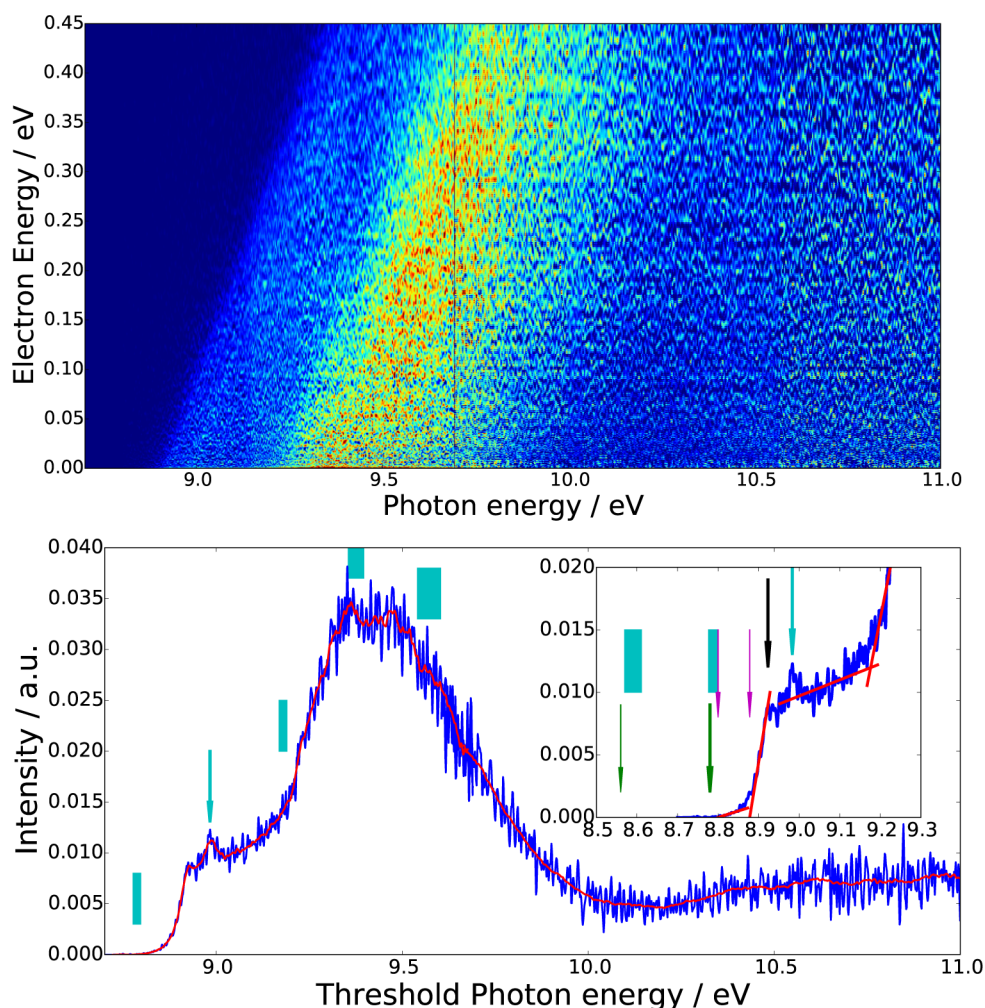


**Figure 3.** (Top) SPES matrix for the total ionization signal in coincidence with the mass of the benzophenone molecular ion. (Bottom) corresponding SPES spectrum in the limit of the first 100 meV kinetic electron energy. The inset corresponds to a zoom of the threshold region. Stick arrows are vertical ionization energies (green, theory; black, experiment). Thin arrows are adiabatic ionization energies (green, theory; magenta, experiment). The cyan arrow is the peak attributed to the C=O stretch. Cyan boxes show the expected locations of the corresponding overtones (see text for details).

**Table 2. Calculated Ionization Energies (eV) of the Benzophenone Molecule Compared to the Experimental Values**

	state	RCCSD(T)	DFT/PBE0	MP2	experiment	
		cc-pVDZ	aug-cc-pVTZ	aug-cc-pVTZ	present work	previous works
adiabatic	$^2D_0$	8.56	8.51		$8.80 \pm 0.01^a$	$9.05^{10}$
					$8.878 \pm 0.005^b$	$9.46 \pm 0.05^{11}$
vertical	$^2D_0$	8.78			$8.923 \pm 0.005$	
adiabatic	$^2D_1$			9.31	$9.17 \pm 0.02$	

<sup>a</sup>Extrapolation of the tail. <sup>b</sup>Extrapolation of the sharp rise.

here that is consistent with the interpretation given below to the sharp peak observed at  $8.983 \pm 0.005$  eV.

The sharp peak that has just been mentioned appears at  $8.8$  eV +  $1476 \pm 50$  cm<sup>-1</sup>. In the range  $1500$ – $1800$  cm<sup>-1</sup>, the C=O or C=C stretches are good candidates for the attribution of this peak. Considering, for example, C=O, the calculated value for this harmonic vibration is  $1667$  cm<sup>-1</sup> (Table SM-1, Supporting Information). Given a scaling factor of  $0.9$  to account for the anharmonicity,<sup>43</sup> the later value is reduced to  $1500$  cm<sup>-1</sup>. The cyan rectangles in Figure 3 show the regions where the overtones of this vibration would be expected, assuming a vibration frequency in the range  $1667$ – $1500$  cm<sup>-1</sup>.

It is not fully conclusive but seems nevertheless self-consistent. The assumption that the sharp peak at  $8.983 \pm 0.005$  eV is the AIE +  $\nu_{C=O}^1$  transition, would also step down the AIE in the range  $8.78$ – $8.80$  eV. This assignment is also in favor of the lowest AIE proposed.

At higher energies, the spectrum is composed of broad and almost structureless bands. These bands correspond to the population of the ground and the lowest doublet states of the benzophenone cation. Such a broad unstructured spectrum is expected for molecules having a large number of low frequency modes (Table SM-1, Supporting Information), which cannot be resolved by the present experiment.

The AIE has also been computed by different theoretical methods as well as the vertical ionization energy. In Table 2 are collected the IEs calculated by the coupled cluster method RCCSD(T)/cc-pVDZ and the DFT method PBE0/aug-cc-pVTZ for the doublet states of the ions. The energy of the optimized geometry of the first excited state calculated with the MP2/aug-cc-pVTZ method is indicated as well. We find that the computed doublet adiabatic values are lower by about 0.2 eV for both methods compared to the present experimental results. Also the  $\sim 0.2$  eV difference between the adiabatic and vertical values for the IE agrees with present experimental observations where the onset to ionization is direct.

**Excited States of the Benzophenone Cation.** A second group of excited states of the benzophenone ion starts at  $9.17 \pm 0.02$  eV (AIE +  $0.37 \pm 0.02$  eV) just above the ground state ion. This group looks to be composed of several broad structures, two of them peaking at  $9.36 \pm 0.01$  eV (AIE +  $0.56 \pm 0.01$  eV) and  $9.47 \pm 0.01$  eV (AIE +  $0.67 \pm 0.01$  eV). A second rise in the SPES spectrum at about  $10.3 \pm 0.1$  eV (AIE +  $1.5 \pm 0.1$  eV) probes another group of excited states.

To interpret the photoelectron spectra, we calculated the transitions to the 8 first excited states at the ground state ion equilibrium geometry. The energies are shown in Table 3. The

**Table 3. Energies (eV) of the Cation Excited States with Respect to the Energy of the Ground State Ion<sup>a</sup>**

states	active space 1		active space 2	experiment	
	CASSCF	MRCI	CASSCF	present work	previous work <sup>10</sup>
<sup>2</sup> D <sub>0</sub>	0	0	0	0	0
<sup>2</sup> D <sub>1</sub>	0.97	0.99	0.85	$0.56^b/0.80^c \pm 0.01$ eV	0.4
<sup>2</sup> D <sub>2</sub>	1.48	1.30	0.99	$0.67^b/0.91^c \pm 0.01$ eV	0.6
<sup>2</sup> D <sub>3</sub>	2.09	1.89	1.74	$1.5^b/1.74^c \pm 0.1$ eV	0.7
<sup>2</sup> D <sub>4</sub>	3.64	3.82	3.56		2.73
<sup>2</sup> D <sub>5</sub>	4.59	4.63	4.09		3.05
<sup>2</sup> D <sub>6</sub>	4.71	4.84	4.60		3.55
<sup>2</sup> D <sub>7</sub>	5.25	5.09	4.99		5.15

<sup>a</sup>Active space 1 = 8 active orbitals. Active space 2 = 10 active orbitals. See text for more details. <sup>b</sup>With respect to the measured AIE at  $8.80 \pm 0.01$  eV. <sup>c</sup>With respect to the calculated AIE at 8.56 eV.

energies were calculated at the CASSCF and MRCI levels, with an active space composed of 8 active orbitals (active space 1). The CASSCF calculations were also performed with a larger active space composed of 10 active orbitals (active space 2). We mainly observe two groups of states: below  $\sim 2$  eV and above  $\sim 3.8$  eV. The first group is likely to interpret the first experimental structure observed: <sup>2</sup>D<sub>1</sub> and <sup>2</sup>D<sub>2</sub> fit with the broad structure spreading from  $9.17 \pm 0.02$  eV to  $\sim 10.0$  eV, and peaking at 9.36 eV (AIE +  $0.56 \pm 0.01$  eV) and 9.47 eV (AIE +  $0.67 \pm 0.01$  eV). <sup>2</sup>D<sub>3</sub> fits with the signal rise at 10.3 eV (AIE +  $1.5 \pm 0.1$  eV). Calculated values are here higher than the experimental ones, but as seen in Table 3, the increase of the active space has a strong influence on the energies.

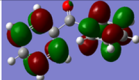
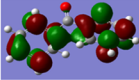
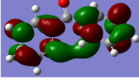
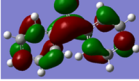
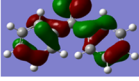
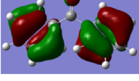
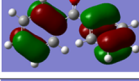
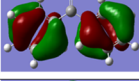
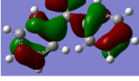
Table 3 reveals that the agreement between the calculated excitation energies of the ion is fair only when the AIE determined experimentally at  $8.80 \pm 0.01$  eV is used. In contrast, it is excellent when the calculated value at 8.56 eV is used. This is an indication that the AIE could be even lower than the value estimated above, when the sharp peak at  $8.983 \pm 0.005$  eV is the first overtone above the 0–0 transition.

Accordingly, it might be the second overtone or it could be associated with a combination of modes implying the C=O and C—C stretch vibrations. However, despite the high quality of the calculations performed on such a large molecule, we do not expect such a close agreement in energy. Including the limitation of the active space size and the usual gap observed between calculated and measured ionization energies, we consider that the present calculations suggest the AIE to be the lowest one measured from the experiment, i.e.,  $8.80 \pm 0.01$  eV.

The vibrational assignment as well as the calculations seems to converge to the AIE value of  $8.80 \pm 0.01$  eV, which we advise for use.

The calculated orbitals of the neutral benzophenone molecule are reported in Table 4. The decomposition of the

**Table 4. Energies, Space Symmetry, and Schematic Representation of the Outermost Molecular Orbitals of Neutral Benzophenone As Deduced at the PBE0/6-31+g(d) Level**

Molecular orbital	Space symmetry C <sub>2</sub> point group	Energy / atomic units	Schematic representation
LUMO + 3	b	-0.01076	
LUMO + 2	a	-0.01917	
LUMO + 1	a	-0.02509	
LUMO	b	-0.06941	
HOMO	b	-0.26514	
HOMO - 1	b	-0.27657	
HOMO - 2	a	-0.27797	
HOMO - 3	a	-0.28101	
HOMO - 4	b	-0.28306	

ionic states onto these orbitals is presented in Table 5, for a comparison between the ground state electronic structure of the neutral molecule and the ones of the electronic states reached by ionization. From this decomposition, it appears that the <sup>2</sup>D<sub>0</sub> state has a strong  $n^{-1}$  character, <sup>2</sup>D<sub>3</sub> is mainly a  $\pi^{-1}$  state and the <sup>2</sup>D<sub>2</sub> and <sup>2</sup>D<sub>1</sub> states are a mixing of  $n^{-1}$  and  $\pi^{-1}$ . Starting from the <sup>2</sup>D<sub>4</sub> state, the structure is somehow different, because it involves the promotion of an HOMO electron into the LUMO state which is the  $\pi_{\text{CO}}^*$  state. Thus, the <sup>2</sup>D<sub>4</sub> state shows an  $n^{-2}\pi_{\text{CO}}^*$  character that may drive the reactivity (i.e., fragmentation) of the ion. <sup>2</sup>D<sub>5</sub>–<sup>2</sup>D<sub>7</sub> states correspond to the

Table 5. Result of the CI Calculation<sup>a</sup>

state	energy (eV)	(HOMO-4) <sup>-1</sup>	(HOMO-3) <sup>-1</sup>	(HOMO-2) <sup>-1</sup>	(HOMO-1) <sup>-1</sup>	(HOMO) <sup>-1</sup>	(HOMO) <sup>-2</sup> (LUMO) <sup>1</sup>
<sup>2</sup> D <sub>0</sub>	0.00				0.67	0.62	
<sup>2</sup> D <sub>1</sub>	0.99		0.44	-0.40	-0.48	0.47	
<sup>2</sup> D <sub>2</sub>	1.30		-0.49	0.45	-0.39	0.45	
<sup>2</sup> D <sub>3</sub>	1.89		0.59	0.65			
<sup>2</sup> D <sub>4</sub>	3.82	0.56					-0.54

<sup>a</sup>We give the weight of the configuration on the corresponding wavefunction quoted at the optimized geometry of the neutral molecule (see text for details).

removal of one electron from the outermost molecular orbital combined with the promotion of one electron into the LUMO.

A further confirmation of the calculated threshold will be given in a forthcoming paper treating the mechanism of the state-to-state unimolecular decomposition of the benzophenone cation.

## CONCLUSION

We photoionized jet cooled benzophenone using VUV synchrotron light. The spectra are assigned by the help of ab initio computations performed on the ground states and on the excited states of the cationic molecule. Structures were optimized. Our calculations show that, in the benzophenone ion, the positive charge becomes localized on one moiety of the molecule. The molecular symmetry switches from C<sub>2</sub> to C<sub>1</sub>. Hence the molecule is on the way to dissociate in a neutral and ionic fragment. We did not find in the literature such examples reported for ionic structures. Hence we can consider the benzophenone ion as a model for the charge localization, in view of this important phenomenon in proteins. Positive charge localization and its migration is a key phenomenon for their integrity and stability, which study has been initiated in the gas phase by Weinkauff et al.<sup>44</sup>

As a consequence, the SPES spectrum of the molecule is quite congested and the adiabatic ionization energies are not unambiguously measured; nevertheless, the ionization threshold is estimated at 8.80 ± 0.01 eV.

## ASSOCIATED CONTENT

### Supporting Information

Vibrational energies of the benzophenone molecule and ion. This material is available free of charge via the Internet at <http://pubs.acs.org/>.

## AUTHOR INFORMATION

### Corresponding Authors

\*M. Hochlaf. E-mail: Majdi.Hochlaf@u-pem.fr.

\*L. Poisson. E-mail: lionel.poisson@cea.fr.

### Notes

The authors declare no competing financial interest.

## ACKNOWLEDGMENTS

We acknowledge SOLEIL for provision of synchrotron radiation facilities and we thank Dr. Gustavo Garcia and Jean-François Gil for assistance in using beamline DESIRS. We are indebted to the general technical staff of Synchrotron Soleil for running the facility under project No. 20120540. We thank Dr. Laurent Nahon, DESIRS beamline director. G.S. thanks EU-ITN project ICONIC-238671 for funding. We thank Dr. Aude Lietard and Dr. Giovanni Piani for help during the acquisition.

We acknowledge the seventh European Community Framework Program under COST ACTION CM1405 MOLIM.

## REFERENCES

- (1) Hochstrasser, R. M.; Lutz, H.; Scott, G. W. The dynamics of populating the lowest triplet state of benzophenone following singlet excitation. *Chem. Phys. Lett.* **1974**, *24*, 162–167.
- (2) Aloise, S.; Rehault, J.; Moine, B.; Poizat, O.; Buntinx, G.; Lokshin, V.; Vales, M.; Samat, A. Photochromism of photoenolizable ketones in quinoline and 1,8-naphthyridine series studied by time-resolved absorption spectroscopy. *J. Phys. Chem. A* **2007**, *111*, 1737–1745.
- (3) Spighi, G.; Gaveau, M.-A.; Mestdag, J.-M.; Poisson, L.; Soep, B. Gas phase dynamics of triplet formation in benzophenone. *Phys. Chem. Chem. Phys.* **2014**, *16*, 9610–9618.
- (4) Murata, R.; Yago, T.; Wakasa, M. Cyclization Reaction of diarylethene through the triplet excited state. *Bull. Chem. Soc. Jpn.* **2011**, *84*, 1336–1338.
- (5) Matsui, Y.; Kido, T.; Ohta, E.; Ikeda, H. The “excited state C-C bond cleavage-luminescence” phenomenon of a biphenyl-substituted methylenecyclopropane triggered by intermolecular energy transfer from triplet benzophenone. *Chem. Commun.* **2014**, *50*, 13963–13966.
- (6) Holtzclaw, K. W.; Pratt, D. W. Prominent, and restricted, vibrational state mixing in the fluorescence excitation spectrum of benzophenone. *J. Chem. Phys.* **1986**, *84*, 4713–4715.
- (7) Bezrodnaya, T. V.; Mel'nik, V. I.; Puchkovskaya, G. A.; Savranskii, L. I. Vibrational and electronic spectra of benzophenone in different phase states: Ab initio calculations and experiment. *J. Struct. Chem.* **2006**, *47*, 194–199.
- (8) Sett, P.; Misra, T.; Chattopadhyay, S.; De, A. K.; Mallick, P. K. DFT calculation and Raman excitation profile studies of benzophenone molecule. *Vibr. Spectrosc.* **2007**, *44*, 331–342.
- (9) Hoffmann, R.; Swenson, J. R. Ground- and excited-state geometries of benzophenone. *J. Phys. Chem.* **1970**, *74*, 415–420.
- (10) Centineo, G.; Fragala, I.; Bruno, G.; Spampinato, S. Photoelectron-spectroscopy of benzophenone, acetophenone and their ortho-alkyl derivatives. *J. Mol. Struct.* **1978**, *44*, 203–210.
- (11) Natalis, P.; Franklin, J. L. Ionization and dissociation of diphenyl and condensed ring aromatics by electron impact. 2. Diphenylcarbons and ethers. *J. Phys. Chem.* **1965**, *69*, 2943.
- (12) Garcia, G. A.; de Miranda, B. K. C.; Tia, M.; Daly, S.; Nahon, L. DELICIOUS III: A multipurpose double imaging particle coincidence spectrometer for gas phase vacuum ultraviolet photodynamics studies. *Rev. Sci. Instrum.* **2013**, *84*, 053112.
- (13) Nahon, L.; de Oliveira, N.; Garcia, G. A.; Gil, J.-F.; Pilette, B.; Marcouille, O.; Lagarde, B.; Polack, F. DESIRS: a state-of-the-art VUV beamline featuring high resolution and variable polarization for spectroscopy and dichroism at SOLEIL. *J. Synchrotron. Rad.* **2012**, *19*, 508–520.
- (14) Richard-Viard, M.; Delboulb , A.; Vervloet, M. Experimental study of the dissociation of selected internal energy ions produced in low quantities: application to N<sub>2</sub>O<sup>+</sup> ions in the Franck-Condon gap and small ionic water clusters. *Chem. Phys.* **1996**, *209*, 159.
- (15) Mercier, B.; Compin, M.; Prevost, C.; Bellec, G.; Thissen, R.; Dutuit, O.; Nahon, L. Experimental and theoretical study of a differentially pumped absorption gas cell used as a low energy-pass



filter in the vacuum ultraviolet photon energy range. *J. Vac. Sci. Technol. A* **2000**, *18*, 2533–2541.

(16) Garcia, G. A.; Nahon, L.; Powis, I. Two-dimensional charged particle image inversion using a polar basis function expansion. *Rev. Sci. Instrum.* **2004**, *75*, 4989–4996.

(17) Pouilly, J. C.; Schermann, J. P.; Nieuwjaer, N.; Lecomte, F.; Gregoire, G.; Desfrancois, C.; Garcia, G. A.; Nahon, L.; Nandi, D.; Poisson, L.; et al. Photoionization of 2-pyridone and 2-hydroxypyridine. *Phys. Chem. Chem. Phys.* **2010**, *12*, 3566–3572.

(18) Briant, M.; Poisson, L.; Hochlaf, M.; de Pujo, P.; Gaveau, M.-A.; Soep, B. Ar<sub>2</sub> Photoelectron spectroscopy mediated by autoionizing states. *Phys. Rev. Lett.* **2012**, *109*, 193401.

(19) Majdi, Y.; Hochlaf, M.; Pan, Y.; Lau, K.-C.; Poisson, L.; Garcia, G. A.; Nahon, L.; Al-Mogren, M. M.; Schwell, M. Theoretical and experimental photoelectron spectroscopy characterization of the ground state of thymine cation. *J. Phys. Chem. A* **2015**, DOI: 10.1021/jp510716c.

(20) Hochlaf, M.; Pan, Y.; Lau, K.-C.; Majdi, Y.; Poisson, L.; Garcia, G. A.; Nahon, L.; Al Mogren, M. M.; Schwell, M. Vibrationally resolved photoelectron spectroscopy of electronic excited states of DNA bases: Application to the state of thymine cation. *J. Phys. Chem. A* **2015**, *119*, 1146–1153.

(21) Adamo, C.; Barone, V. Toward reliable density functional methods without adjustable parameters: The PBE0 model. *J. Chem. Phys.* **1999**, *110*, 6158–6170.

(22) Frisch, M. J.; Trucks, G. W.; Schlegel, H. B.; Scuseria, G. E.; Robb, M. A.; Cheeseman, J. R.; Scalmani, G.; Barone, V.; Mennucci, B.; Petersson, G. A.; et al. *Gaussian 09*, revision A.02; Gaussian Inc.: Wallingford, CT, 2009.

(23) Dunning, T. H. Gaussian-basis sets for use in correlated molecular calculations. I. the atoms boron through neon and hydrogen. *J. Chem. Phys.* **1989**, *90*, 1007–1023.

(24) Kendall, R. A.; Dunning, T. H.; Harrison, R. J. Electron affinities of the first row atoms revisited. systematic basis sets and wave functions. *J. Chem. Phys.* **1992**, *96*, 6796–6806.

(25) Møller, C.; Plesset, M. S. Note on an approximation treatment for many-electron systems. *Phys. Rev.* **1934**, *46*, 618–622.

(26) Hampel, C.; Peterson, K. A.; Werner, H.-J. A comparison of the efficiency and accuracy of the quadratic configuration interaction (QCISD), coupled cluster (CCSD), and Brueckner coupled cluster (BCCD) methods. *Chem. Phys. Lett.* **1992**, *190*, 1–12.

(27) Deegan, M. J. O.; Knowles, P. J. Perturbative corrections to account for triple excitations in closed and open shell coupled cluster theories. *Chem. Phys. Lett.* **1994**, *227*, 321–326.

(28) Knowles, P. J.; Hampel, C.; Werner, H.-J. Coupled cluster theory for high spin open shell reference wavefunctions. *J. Chem. Phys.* **1993**, *99*, 5219–5227.

(29) Knowles, P. J.; Hampel, C.; Werner, H. J. Coupled cluster theory for high spin, open shell reference wave functions (vol 99, pg 5219, 1993). *J. Chem. Phys.* **2000**, *112*, 3106–3107.

(30) Watts, J. D.; Gauss, J.; Bartlett, R. J. Coupled-cluster methods with noninterative triple excitations for restricted open-shell Hartree-Fock and other general single determinant reference functions - Energies and analytical gradients. *J. Chem. Phys.* **1993**, *98*, 8718–8733.

(31) Werner, H.-J.; Knowles, P.; Knizia, G.; Manby, F.; Schütz, M.; Celani, P.; Korona, T.; Lindh, R.; Mitrushenkov, A.; Rauhut, G.; et al. *MOLPRO*, version 2012.1, a package of ab initio programs, 2012; <http://www.molpro.net/>.

(32) Knowles, P. J.; Werner, H.-J. An efficient second order MCSCF method for long configuration expansions. *Chem. Phys. Lett.* **1985**, *115*, 259–267.

(33) Werner, H.-J.; Knowles, P. J. A second order MCSCF method with optimum convergence. *J. Chem. Phys.* **1985**, *82*, S053.

(34) Knowles, P. J.; Werner, H.-J. An efficient method for the evaluation of coupling coefficients in configuration interaction calculations. *Chem. Phys. Lett.* **1988**, *145*, 514–522.

(35) Werner, H.-J.; Knowles, P. J. An efficient internally contracted multiconfiguration reference CI method. *J. Chem. Phys.* **1988**, *89*, 5803–5814.

(36) Fleischer, E. B.; Sung, N.; Hawkinson, S. Crystal structure of benzophenone. *J. Phys. Chem.* **1968**, *72*, 4311–4312.

(37) Coon, J. B.; Cesani, F. A.; Huberman, F. P. 2491 Å absorption systems of NO<sub>2</sub> and a double-minimum potential. *J. Chem. Phys.* **1970**, *52*, 1647.

(38) Hallin, K. E. J.; Merer, A. J. 2491 Å band system of NO<sub>2</sub> - Rotational structure and evidence for predissociation in zero-point level. *Can. J. Phys.* **1976**, *54*, 1157–1171.

(39) Schinke, R.; Grebenshchikov, S. Y.; Zhu, H. The photodissociation of NO<sub>2</sub> in the second absorption band: Ab initio and quantum dynamics calculations. *Chem. Phys.* **2008**, *346*, 99–114.

(40) Upadhyaya, H. P.; Kumar, A.; Naik, P. D. Photodissociation dynamics of enolic-acetylacetone at 266, 248, and 193 nm: Mechanism and nascent state product distribution of OH. *J. Chem. Phys.* **2003**, *118*, 2590–2598.

(41) Poisson, L.; Roubin, P.; Coussan, S.; Soep, B.; Mestdag, J. M. Ultrafast Dynamics of Acetylacetone (2,4-Pentanedione) in the S<sub>2</sub> State. *J. Am. Chem. Soc.* **2008**, *130*, 2974–2983.

(42) Milosavljević, A. R.; Kočišek, J.; Papp, P.; Kubala, D.; Marinković, B. P.; Mach, P.; Urban, J.; Matejčík, S. Electron impact ionization of furanose alcohols. *J. Chem. Phys.* **2010**, *132*, 104308.

(43) Leš, A.; Adamowicz, L.; Nowak, M. J.; Lapinski, L. The infrared spectra of matrix isolated uracil and thymine: An assignment based on new theoretical calculations. *Spectrochim. Acta A* **1992**, *48*, 1385–1395.

(44) Weinkauff, R.; Schanen, P.; Metsala, A.; Schlag, E. W.; Bürgle, M.; Kessler, H. Highly efficient charge transfer in peptide cations in the gas phase: threshold effects and mechanism. *J. Phys. Chem.* **1996**, *100*, 18567–18585.